Taguchi Optimization of TiO_2 Thin Film to Defeat Microbiologically Induced Corrosion of Stainless Steel

Hooman Baghi Baghban [1], Sanaz Naghibi [2,*]

[1] MSc graduated students, Department of Technical and Engineering, Shahreza Branch, Islamic Azad University, Shahreza, Iran.

[2] Assistant professor, Department of Technical and Engineering, Shahreza Branch, Islamic Azad University, Shahreza, Iran.

ARTICLE INFO

Article history:

Received 24 May 2018
Accepted 18 November 2018
Available online 15 June 2019

Keywords:

Microbiologically induced corrosion
TiO_2
Thin film
Taguchi method
Steel

ABSTRACT

Although microbiologically induced corrosion (MIC) is well known by design engineers and manufacturers, most current marine devices continue to be impressed by MIC. This phenomenon originates from colonization of anaerobic microorganisms on metal surface, and subsequently increases the corrosion rate. An investigation was made to defeat MIC by means of applying a TiO_2 thin film on metal surface. 316L stainless steel and sol-gel dipping technique were chosen as the base metal and application method, respectively. The depositing variables including PEG adding amount, pH of the sol, calcination temperature (T), and dipping cycles number, were analyze by Taguchi statistical model to determine their influences on response parameters: bactericidal efficiency, current corrosion density (i_{corr}), crystallinity, crystallite size, and surface roughness (R_a). A parameter termed *Aim* was defined to comprise all the response parameters. Taguchi Predicted conditions to achieve the highest *Aim* value. For this aim, PEG content, pH, T, and dipping cycles should be equal to 1 g per 100 mL of sol, 11, 600 °C, and 2 cycles, respectively. These conditions were applied to prepare the optimized sample. Careful evaluation of this sample approved the Taguchi prediction and the highest *Aim* value was observed.

1-Introduction

Microbiological corrosion is one of the most critical problems in marine devices and equipment and induces demolition of structures and/or components, stoppage of machinery, and consequently huge economic loss [1-3]. Stainless steel due to its unique characteristics, finds various applications in marine and port industries, whereas its microbiological corrosion resistance needs to be improved [1, 4-6]. To tackle this issue, several methods have been introduced, such as using cathodic protection [5], electrochemical techniques [1], biopolymer [4], inhibitor agent [6, 7], UV irradiation [8], and molecular microbiological methods [9]. A general and inexpensive but effective solution is to isolate the metal surface from corrosive media by applying persistent and resistant coatings that could be ceramics, polymers, alloys or composites [10-14]. TiO_2 as an oxide ceramic with high chemical and thermal stability, low electrical conductivity and poor thermal expansion, is one of the most studied material to be applied as an anticorrosion

* Corresponding author:
E-mail address: naghibi@iaush.ac.ir

thin film [15, 16], or a reinforcing agent in polymer coatings [17]. On the other hand, TiO_2 as a widely used photocatalyst has been preferentially utilized in anti-microbiological corrosion coatings [18-22]. Poulios et al (1999) reported that TiO_2-P25 as a film leads to decrease the rate of sulfation in comparison to bare marble. They dipped marble substrates in an aqueous solution of TiO_2 NPs [18]. Ma et al (2009) used direct current electrodeposition method to apply Ni-P-Cr/TiO_2 coating on steel surface. They showed that the existence of TiO_2 NPs in this coating causes its better passive performance and unique antibacterial activity. These characteristics make Ni-P-Cr/TiO_2 coatings able to have excellent antibacterial and corrosion resistance properties [23]. Wang et al (2010) prepared Ce-doped TiO_2 and TiO_2 film on stainless steel via a sol gel method. They showed that the bactericidal efficiency of the coated samples were 95 and 85%, respectively [21]. Wang et al (2011) fabricated N-doped TiO_2 thin film on stainless steel via deposition of TiN film by plasma surface alloying technique and subsequently heating it in air at 450 °C. They reported that the N-doped TiO_2 coating not only had outstanding bactericidal efficiency, but also afforded anticorrosion performance [20]. Basheer et al (2013) chemically modified the galvanization process by addition of W-TiO_2 composite to the hot zinc bath. Accordingly, they prepared W-TiO_2 modified galvanized steel and evaluated its mirobiologically influenced corrosion. The W–TiO_2 incorporated zinc coating limits biofilm-forming during the biofouling process [22].

However, as far as we studied, application of TiO_2 NPs and thin films to improve microbiological corrosion behavior of steel is approximately limited to the mentioned works above and lack of a systematic research in this field is felt. To deal with this issue, two subjects should be considered: deposition technique and research methodology.

Several methods have been reported to deposit a thin film on metal surface such as electrophoretic deposition [24], spray deposition [25], chemical vapor deposition (CVD) [26], physical vapor deposition (PVD) [27], sol-gel based technique [28], etc. However, the last one is considered among the interesting methods due to its potentially ease of apply, lower cost, fewer equipment, and possibility of composition and microstructure control [29]. Heretofore, abundant studies have been conducted to optimize TiO_2 thin film deposited via sol gel dipping technique [30-32]. In these works, as well as in other similar researches, a few valuables have been studied. To cope with this issue, statistical research methods have been developed to simultaneously analyze three or more variables [33-35]. Taguchi optimization approach is one of the most powerful and well-known statistical techniques which has been utilized for optimizing preparation parameters in material science field such as welding [36], drilling [37], forming [38], nanoparticles synthesizing [39-41], biomaterials [42], and thin film depositing [43, 44]. This method is aimed on studying multiple variables with carrying out minimum number of experimental runs [45]. TiO_2 thin film preparation has previously been optimized by this approach to improve its corrosion behavior [15], photocatalytic performance [46], permeate flux and chemical oxygen demand removal [47], and adhesion and wear behavior [48].

This work focused on optimization of TiO_2 thin film deposition over stainless steel substrate to improve its microbial induced corrosion resistance. The deposition process was carried out based on the sol gel dipping technique. For this aim, Taguchi approach was utilized to design the experimental procedure and four variables, i.e. PEG adding amount, pH of the sol, calcination temperature, and dipping cycle's number, were selected as the preparation parameters. The other parameters of the process were selected constant.

2- Experimental Procedure

2-1- Taguchi experimental design

Taguchi L9 orthogonal array plan was opted out to design the experimental procedure of TiO_2 thin film preparation. The PEG amount, pH of the sol, calcination temperature, and dipping cycle's number were defined as independent variables with three levels. Table 1 provided the variables with their levels and Table 2 represented series of runs to prepare the required samples. Analysis of *signal-to-noise* (S/N) ratio and *mean of means* were performed to determine significant variables. MINITAB-14 statistical software was used for regression analysis and to draw S/N ratio plots.

Table 1. Preparation conditions: variables and their levels, and constant parameters.

Variables	**Level 1**	**Level 2**	**Level 3**
PEG adding amount (g/100 mL of the sol)	0	1	2
pH of the sol	7	9	11
Calcination temperature (°C)	400	500	600
Dipping cycles number	2	6	10
Constants			
Substrate	316L stainless steel; 20*20*2 mm^3		
Ti-precursor	Titanium tetraisopropoxide (TTIP)		
Deposition method	Dip coating		
Immersion and withdrawal speed	1.7 mm per second		
Immersion time	1 min		

Table 2. Series of runs to prepare the samples.

Sample		**1**	**2**	**3**	**4**	**5**	**6**	**7**	**8**	**9**
Variables	PEG adding amount (g/100 mL of the sol)	0	0	0	1	1	1	2	2	2
	pH of the sol	7	9	11	7	9	11	7	9	11
	Calcination temperature (°C)	400	500	600	500	600	400	600	400	500
	Dipping cycles number	2	6	10	10	2	6	6	10	2

2-2- Sol preparation and thin film deposition

The starting chemicals, i.e. titanium tetraisopropoxide (TTIP), isopropyl alcohol (iPrOH), hydro chloric acid (HCl), three ethylamine (TEA), and poly ethylene glycol (PEG, 6000 g/mol) were purchased from Merck and used without purification.

75 mL of TTIP was dissolved in 75 mL of iPrOH and stirred for an hour, and then 900 mL of distilled water was dropwise added to TTIP/iPrOH solution and rigorously stirred for 30 min. pH of the solution was adjusted to 1.5 by addition of adequate amounts of HCl and stirred rigorously for 2 days. This condition was provided to perform the hydrolysis reactions. Next, the as-received solution was poured into 100 mL in 9 beakers. The adequate amounts of PEG were added to some beakers, by taking into account Table 2. The solutions were stirred to dissolve PEG and their pH values were adjusted to reach the required values (according to Table 2) by addition of TEA. The solutions were aged for 48 h at room temperature under continuous stirring before deposition.

Following sandpapering, surface polishing and cleaning, the 316L stainless steel substrate specimens (dimension: 20*20*2 mm^3) designated for thin film deposition were subjected to the as-prepared solutions. The Ti-containing sols were applied on the substrates via the sol-dipping technique with a controlled immersion and withdrawal speed of 1.7 mm per second, and 1 min of immersion time. This process was accomplished by a dip coater machine (109C, Pasargad Nano Equipment, Tehran, Iran). The dipping cycle's number was assigned as the variable parameter and presented in Table 2. The coated specimens were kept 48 h for natural drying. Next, heat treatment was performed by increasing temperature with a heating rate of 2 °C/min to 150 °C, fixing for 30 min, continuing the heating with rate of 5 °C/min to reach the maximum temperatures which are presented in Table 2, and fixing for 1h. The furnace was turned off and cooled with natural rate.

2-3- Bactericidal assay

Bactericidal influences of the as-deposited films on stainless steel substrates were evaluated by using sulfate-reducing bacteria (SRB) as a biocorrosion agent. This type of bacteria was incubated at 25 °C in the Postgate's medium B. This medium was consisted of KH_2PO_4 (0.5 g/L), NH_4Cl (1 g/L), $CaSO_4$ (1 g/L), $MgSO_4.7H_2O$ (2 g/L), $FeSO_4.7H_2O$ (0.5 g/L), sodium lactate (3.5 g/L), yeast extract (1 g/L), ascorbic acid (1 g/L), thioglycolic acid (0.1 g/L),

and distilled water. The pH value was adjusted to 7.2 using NaOH or HCl, and $FeSO_4$ was used to detect H_2S produced by SRB. This suspension should be sterilized by autoclaving at 121 °C and 1.2 atm for 15 min, and deoxygenized. The incubated SRB suspension was kept in an incubator at 37 °C for 4 days, and then diluted 10^4 times with deionized water to facilitate growth and also counting of bacteria. 25 µL of the diluted SRB suspension was pipetted on the bare and coated samples, and then 1 mL of distilled water was poured around it to assure ~ 100% relative humidity. The samples were placed in a vacuum chamber to provide anaerobic conditions and then exposed to UV irradiation for 1 h (2 UV lamps, distance=10 cm, λ=365 nm, P=15 W, Philips). The irradiated SRB suspensions were washed by distilled water and poured into Petri dishes. Nutrient agar solution was added to the Petri dishes and covered with preservative parafilm (plastic paraffin film) to prevent the passage of air. The petri dished were placed in an incubator with temperature of 37 °C for 4 days under anaerobic conditions. The viable SRB colonies were counted and considered to calculate the bactericidal efficiency via Eq. 1.

$$\text{Bactericidal efficiency} = \frac{N_B - N_C}{N_B} \times 100 \qquad (1)$$

where N_B is the number of viable SRB on the bare sample and N_C is related to the coated samples after irradiation.

2-4- Corrosion experiments

Tafel polarization test was selected to evaluate the anticorrosive performance of the coatings. The tests were carried out by a potentiostat/galvanostat device (EG&G, model: 237A, USA) in a 3-electrode cell (working electrode, the saturated calomel electrode, and platinum auxiliary electrode) with 0.5 mol/L NaCl solution. In order to compare the samples, the corrosion parameters such as current corrosion density (I_{corr}), corrosion potential (E_{corr}), polarization resistance (R_P), and corrosion rate (CR) were extracted from Tafel curves by Power Suite software.

2-5- Characterizations

The phase analysis of the deposited thin films was accomplished by X-ray diffraction (XRD) method using a Bruker diffractometer (D8 advance) with Cu tube anode and Ni filter. The statistical methods require numerical data; therefore, the XRD results should convert from their descriptive form to the numerical form. The degree of crystallinity and crystallite size were extracted from the XRD patterns. The procedures by which these parameters were measured are explained elsewhere [40].

The morphological imaging of the specimens was performed by field emission scanning electron microscopy (FESEM, 4160, Hitachi, Japan) with acceleration voltage of 15 kV.

The surface topographical imaging of the samples was accomplished by atomic force microscopy (AFM) using a Bruker device (nanos 1.1).

2-6- Definition of Aim parameter

The aim of this work is based on depositing a thin film on steel substrates to overcome microbiologically induced corrosion problem. On the other hand, there are some points to consider in coating a metallic substrate. Corrosion resistance, degree of crystallinity, and surface roughness are parameters determining the quality of the thin film. To simultaneously evaluate the effect of all these parameters, an index was defined in Eq. 2 by the name '*Aim*':

$$Aim = (\text{Bactericidal efficiency}) \times (\text{Corrosion resistance improvement}) \times (\text{Crystallinity}) / (\text{Surface roughness variation}) \qquad (2)$$

Where

$$\text{Corrosion resistance improvement} = \frac{i_{corr}[\text{uncoated}] - i_{corr}[\text{coated}]}{i_{corr}[\text{uncoated}]} \times 100 \qquad (3)$$

$$\text{Surface roughness variation} = \frac{\text{surface roughness}_{\text{coated}}}{\text{surface roughness}_{\text{uncoated}}} \times 100 \qquad (4)$$

3- Results and Discussion

3-1- Analysis of S/N for bactericidal efficiency

The bactericidal efficiency of the samples was calculated and their values are presented in Table 3. The statistical calculation was

performed by MINITAB and the results were presented in Table 4 and Figure 1. Figure 1 shows the interaction and main effects plots for S/N ratios of the bactericidal efficiency. Based on the interaction plot (Figure 1-b), an interaction between the variables is inevitable due to the nonexistence of the parallel lines. Figure 1-b shows mean of means graph. It is obvious that the highest influence on the bactericidal efficiency was related to PEG content. By addition of 1 g of PEG to 100 mL of the sol, the bactericidal efficiency strongly increases. More increase in PEG content leads to moderate decrease bactericidal efficiency. In addition, pH is the second parameter influencing bactericidal behavior. Neutral pH is the best condition to prepare a thin film with the highest bactericidal efficiency. With increase in pH value, the bactericidal efficiency decreases and subsequently slightly increases. The other two parameters (dipping cycle's number and calcination temperature) have less impact on the bactericidal efficiency. Increasing the calcination temperature and decreasing the number of dipping cycles lead to improve the bactericidal efficiency.

Table 3. The extracted numerical data from the different characterization methods (Samples 1-9).

Sample	Bactericidal efficiency (%)	i_{corr} ($\mu A.cm^{-2}$)	Degree of crystallinity (%)	Crystallite size (nm)	R_a (nm)	*Aim* (%)
1	27.6	1.781	52	16	8	26.8
2	13.5	2.242	57	16	10	8.5
3	17.6	1.124	64	25	8	28.9
4	60.0	2.513	61	24	11	29.2
5	58.0	1.267	77	28	15	57.5
6	57.9	0.016	49	18	10	84.7
7	60.0	2.246	85	34	20	28.1
8	21.4	2.578	55	17	11	8.8
9	52.9	1.290	55	18	15	37.1
Bare	3.6	3.551	-	-	-	-

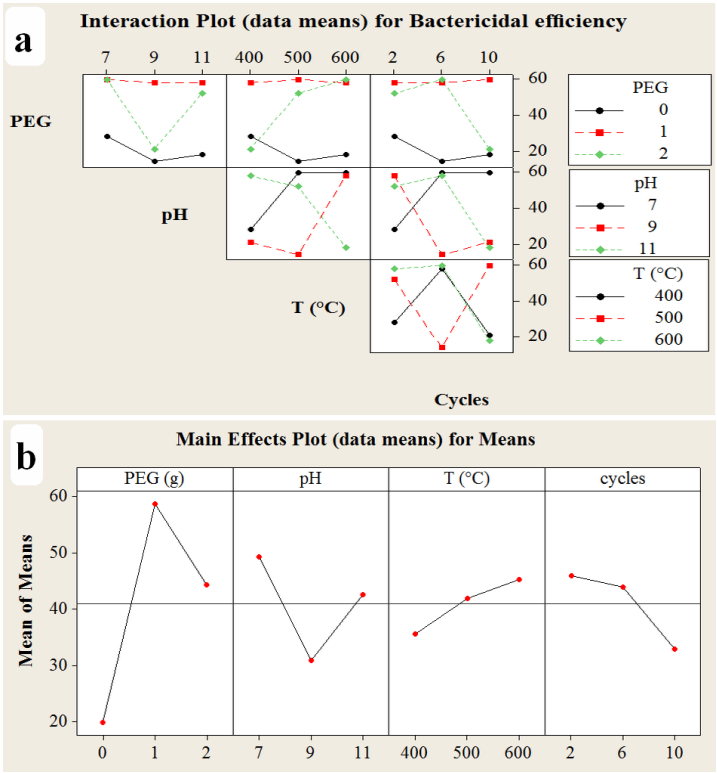

Figure 1. Interaction plot (a) and main effects plot (b) for S/N ratios of the bactericidal efficiency.

Table 4. Response table for means

Response factors ↓	Variables →		PEG adding amount (g/100 mL of the sol)	pH of the sol	Calcination temperature (°C)	Dipping cycles number
Bactericidal efficiency (%)	Level	1	20.00	49.33	35.67	46.00
		2	58.67	31.00	42.00	44.00
		3	44.33	42.67	45.33	33.00
	delta		38.67	18.33	9.67	13.00
	rank		1	2	4	3
i_{corr} ($\mu A.cm^{-2}$)	Level	1	1.72	2.18	1.46	1.45
		2	1.26	2.03	2.02	1.50
		3	2.04	0.81	1.55	2.07
	delta		0.77	1.37	0.56	0.63
	rank		2	1	4	3
Degree of crystallinity (%)	Level	1	57.67	66.00	52.00	61.33
		2	62.33	63.00	57.67	63.67
		3	65.00	56.00	75.33	60.00
	delta		7.33	10	23.33	3.67
	rank		3	2	1	4
Crystallite size (nm)	Level	1	19.00	24.67	17.00	20.67
		2	23.33	20.33	19.33	22.67
		3	23.00	20.33	29.00	22.00
	delta		4.33	4.33	12.00	2.00
	rank		3	2	1	4
R_a (nm)	Level	1	8.67	13.00	9.67	12.67
		2	12.00	12.00	12.00	13.33
		3	15.33	11.00	14.33	10.00
	delta		6.67	2.00	4.67	3.33
	rank		1	4	2	3
Aim (%)	Level	1	21.40	28.03	40.10	40.47
		2	57.13	24.93	24.93	40.43
		3	24.67	50.23	38.17	22.30
	delta		35.73	25.30	15.17	18.17
	rank		1	2	4	3

3-2- Analysis of S/N for current corrosion density

The Tafel polarization graphs and i_{corr} values are presented in Figure 2 and Table 3, respectively. As can be seen, the coated samples are more resistant to corrosion in comparison with the bare sample. These values were used to statistical calculation and to draw the interaction plots and main effects plots for S/N ratios of i_{corr}. Response values for means are summarized in Table 4 and statistical plots are shown in Figure 3.

Figure 3-a shows an interaction between the control variables because of the non- paralleled lines. Figure 3-b shows the statistical analysis. It is clear that pH value is the most influential parameter affecting corrosion behavior of the coated samples. The pH and i_{corr} are in reverse relation. By increasing pH in the range of 9−11, i_{corr} as an index of corrosion of underground metal substrates decreased but improvement was expected. According to Table 4, PEG content hold the second rank among the parameters affecting i_{corr}. The optimum content of PEG which exhibited the lowest i_{corr} is addition of 1 g of PEG to 100 mL of the sol. Two other factors (i.e. calcination temperature and dipping cycle's number) showed less impact on the corrosion behavior. Their best values to achieve the lowest i_{corr} are 400 and 600 °C for calcination temperature and 2 and 6 times for dipping cycles.

As can be seen in the previous sections (3.1. and 3.2.), the bactericidal performance and anticorrosion efficiency of the coated samples are not similar. In order to evaluate these behaviors, samples were characterized by different methods. The aim of this section lies on clarifying relation between the thin films characteristics and their corrosion behavior. For this reason, XRD, FESEM, and AFM were utilized to determine phase component, degree of crystallinity, morphology, and topography of the as-deposited thin films.

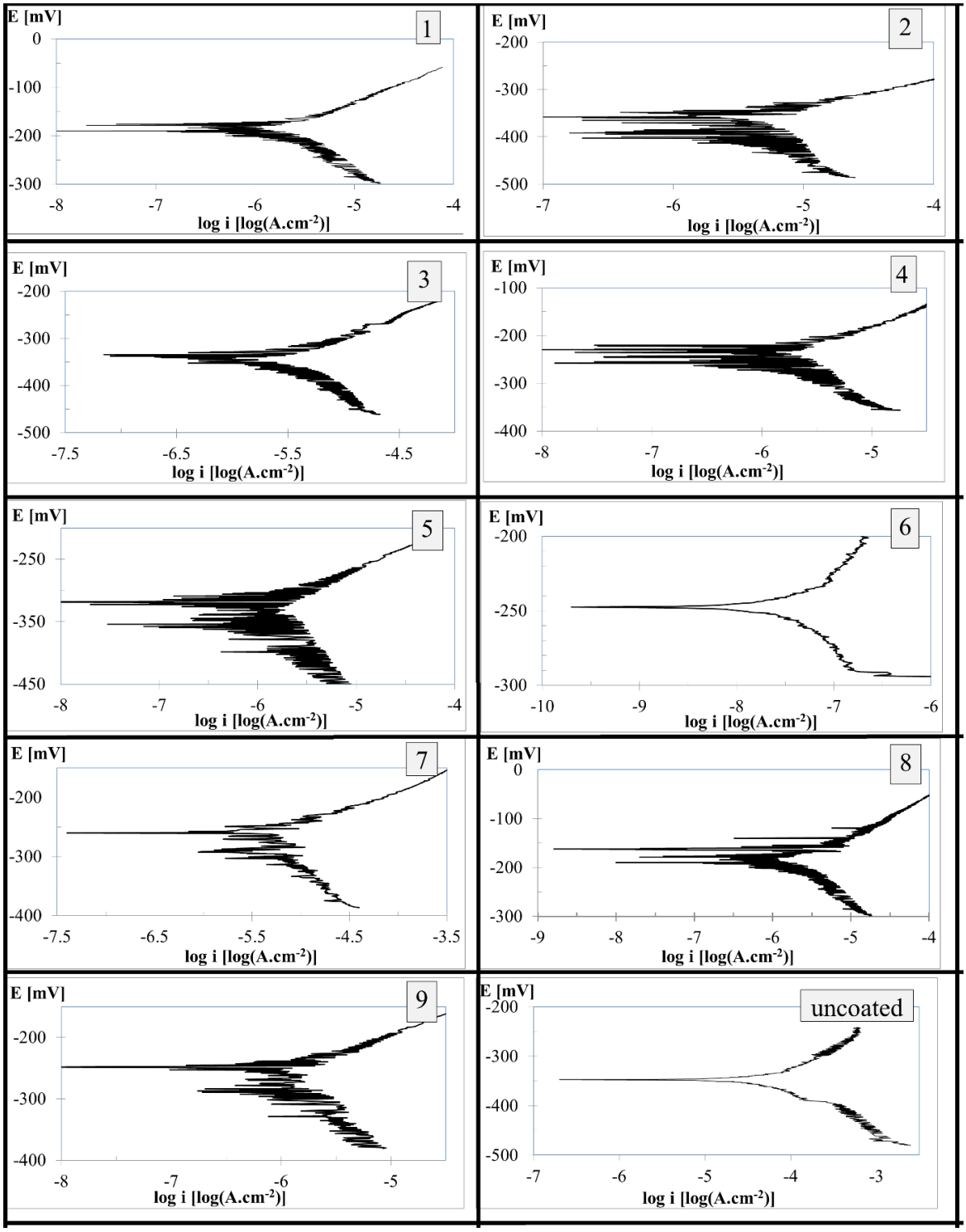

Figure 2. Polarization curves of the samples.

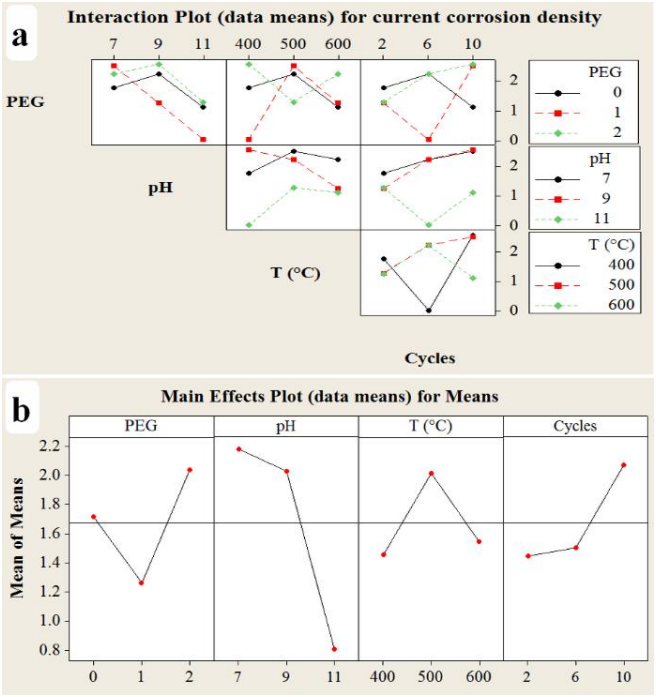

Figure 3. Interaction plot (a) and main effects plot (b) for S/N ratios of the current corrosion density.

3-3- Phase component, crystallinity, crystallite size and surface roughness

Although the processing conditions have no considerable influence on phase component of the samples, it is evident from Figure 4 that width and height of the peaks are not similar. The degree of crystallinity and crystallite size data were extracted from the XRD patterns and presented in Table 3. Another parameter influencing the corrosion behavior is surface roughness (R_a), which is achievable with atomic force microscopy. Although AFM images are not shown here, they are used to calculate R_a values (Table 3). These values were used to statistical calculation and to draw the interaction plots and main effects plots for S/N ratios of crystallinity, crystallite size, and R_a. Response values for means are summarized in Table 4 and statistical plots are shown in Figure 5 and Figure 6. This section would be used to analyze the observations.

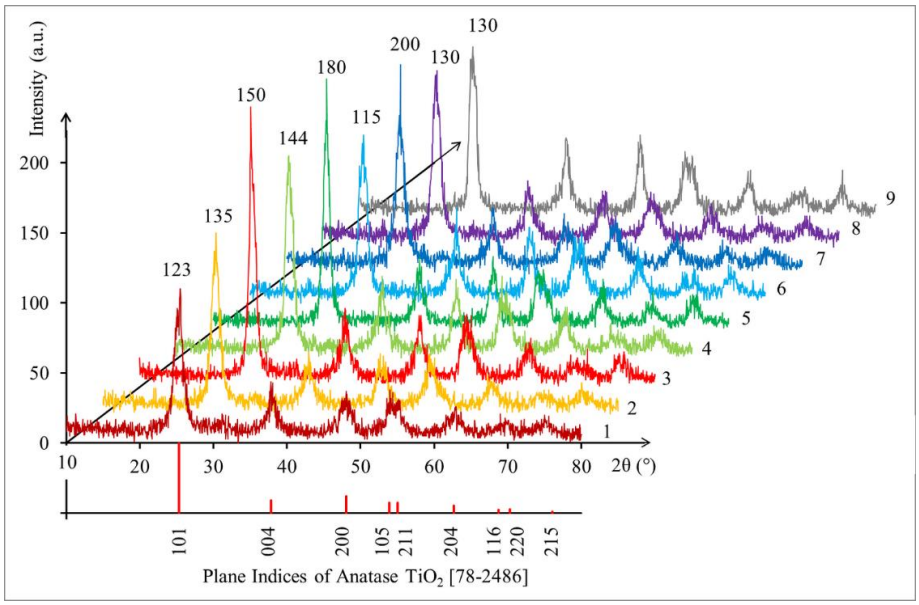

Figure 4. XRD patterns of the as-prepared samples

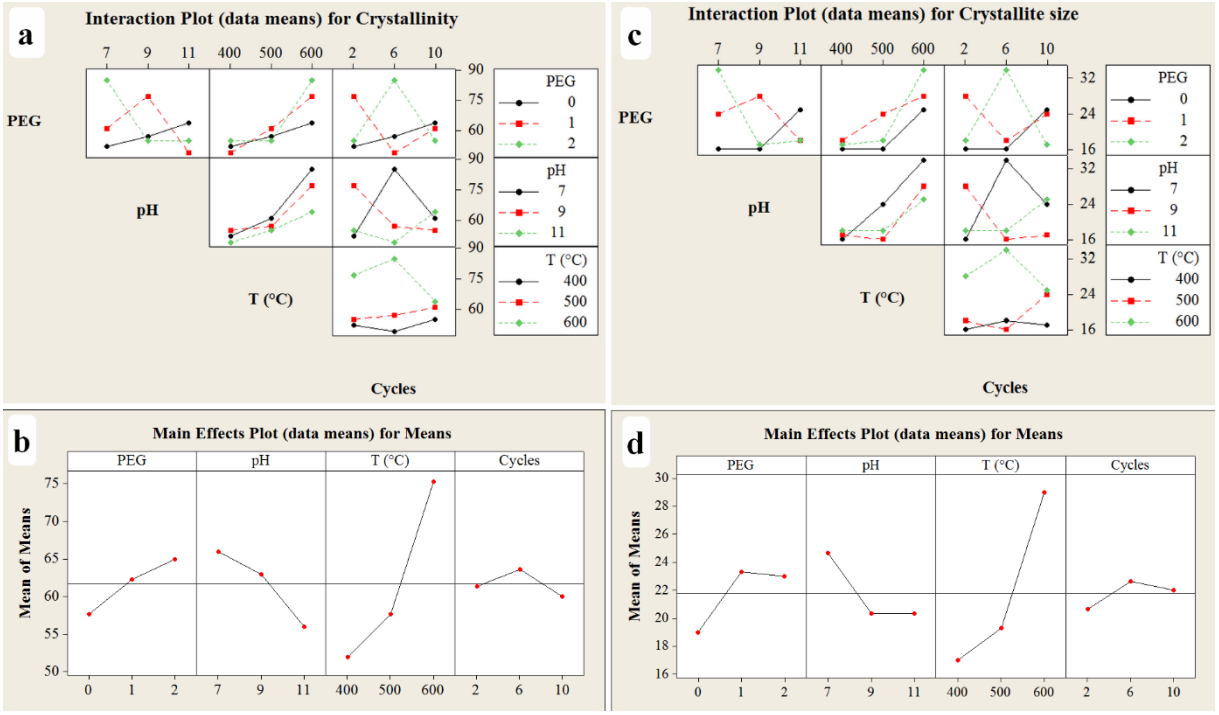

Figure 5. Interaction plot (a) and main effects plot (b) for S/N ratios of the crystallinity. Interaction plot (c) and main effects plot (d) for S/N ratios of the crystallite size.

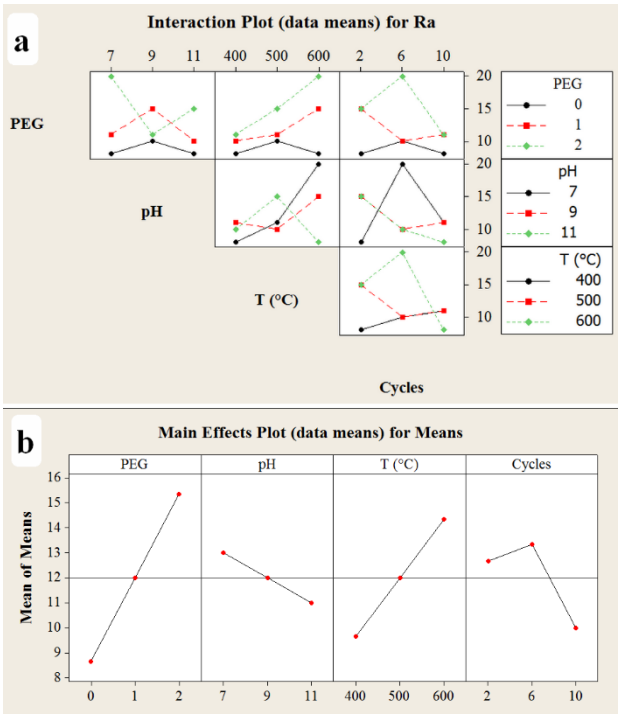

Figure 6. Interaction plot (a) and main effects plot (b) for S/N ratios of R_a.

3-4- Analyzing the observations

Figures 1 and 3 are related to the bactericidal efficiency and i_{corr} values, respectively. It should be mentioned that the "*larger is better*" and "*smaller is better*" were adopted as optimization principle for these parameters, respectively. The optimum PEG content to achieve maximum bactericidal efficiency and minimum i_{corr} value is 1 g. The role of PEG in dip-coating sols is to form a polymeric network which provides

relatively greater green thin film strength, holds the deposited layer together during drying process, and avoids cracks formation. The presence of this polymeric material can be the origin of an important problem; discontinuities. This defect is due to more amount of PEG being added to the sol, and is formed as a result of its burning-out [49]. Micro cracks and discontinuities lead to higher corrosion rates and pitting and also higher microbial-induced corrosion.

The corrosion and microbial corrosion behaviors are also affected by the pH values. Taguchi graphs show that these effects are not similar for the parameters. In the case of i_{orr}, increasing in pH led to decrease in corrosion rate. Whereas in the case of bactericidal efficiency, an increase in pH value from 7 to 9 caused to weaken the efficiency. Meanwhile, further increase to 11 led to slightly improve its performance. Considering Figures 5 and 6 shows that crystallite size, crystallinity, and R_a were decreased with increasing in pH. It seems that surface roughness is the parameter strongly controls i_{corr}, whereas the other parameters (crystallite size andcrystallinity) are also known to have impact on the bactericidal efficiency. At the low pH value (pH=7), the crystallinity has such a high value that it led to improve the bactericidal efficiency. However, increase in pH decreases crystallinity and also the bactericidal efficiency. More increase in pH led to strongly decrease in R_a and crystallite size. It means that specific surface area of the as-deposited film increases and therefore, its bactericidal performance improves.

The influence of the calcination temperature on i_{corr} value is not linear and is inconsistent, as observed in Figure 3, whereas in the case of bactericidal efficiency this relation is linear and positive, as observed in Figure 1. The higher the temperature is, the higher the bactericidal efficiency will be. Briefly, 500 °C is a temperature leads to higher i_{corr}. As can be seen in Figures 5 and 6, increase in calcination temperature from 400 to 500 °C leads to sharp increase in R_a and slight increase in crystallinity. In such a condition, R_a acts as an effective parameter in the intermediate temperature and leads to increase i_{corr}. Furthermore increase in temperature to 600 °C strongly increases the degree of crystallinity and therefore leads to decrease in i_{corr}. However, 400 and 600 °C are the temperatures which are appropriate for this purpose. On the other hand, the optimized calcination temperature to obtain the highest bactericidal efficiency is 600 °C. The correlation between the investigated parameters (bactericidal efficiency and i_{corr}) and the number of dipping cycles is a linear and positive relationship. The more the dipping cycles is, the more the thickness of the thin film will be obtained and therefor the more bactericidal efficiency and the fewer i_{corr} will be achieved.

3-5- Aim parameter

The main aim of this work is to deposit a thin film with good resistance to corrosion and microbiologically induced corrosion problems. In this among, some other parameters also play decisive roles, such as crystallinity and R_a. As described in *Section 2.6.*, the *Aim* parameter was defined, calculated and presented in Table 3. These values were used to statistical calculation and to draw the main effects plots for S/N ratios of *Aim* parameter. Response values for means are summarized in Table 4 and statistical plots are shown in Figure 7. The processing agent which plays the greatest role is the PEG content. As discussed before, addition of 1 g of PEG leads to the highest bactericidal efficiency and anticorrosion performance. The second factor influencing the *Aim* parameter is the pH value. Figure 7 shows that the highest pH value leads to obtain the maximum value of the *Aim* parameter. Preparation of a solution with pH of 11 led to a relatively high bactericidal efficiency and also to a strongly high anticorrosion performance. In the case of calcination temperature, 400 and 600 °C are appropriate temperatures for calcination. Considering Figure 1, 600 °C is selected as the best temperature. Finally, 2 and 6 dipping cycles showed similar results in Figure 7. By according to Figure 1, the optimum number of dipping cycles is selected as 2. Based on these results, the optimum processing parameters to deposit thin film with the desired characteristics are: PEG content of 1 g, pH of 11, calcination temperature of 600 °C, and 2 cycles of dipping. One sample is designed and prepared by according to these conditions, expecting to lead to the deposition of TiO_2 thin film with the highest anticorrosion performance and

bactericidal efficiency. This sample was prepared and evaluated to compare with the other samples and to validate the Taguchi analysis results.

3-6- Evaluation of the optimized sample

Figure 8 shows XRD pattern, SEM image, and AFM graph of the as-prepared optimized sample. XRD analysis approves the formation of anatase as a unique phase in the thin film. It is exactly the same as the phase component of the other synthesized samples. SEM image shows a well-developed and continuous thin film with a nano-crack network. Furthermore, some particles can be observed embedded in the thin film with size of 20-300 nm. AFM image shows that this thin film is consisted of a large number of interconnected particles of approximately 100 nm in size. Noteworthy point is that there is not a trace of the nano- cracks network in the AFM image. This can be attributed to this fact that the observed cracks are shallow and their depths are limited to the thickness created by one cycle of dipping. However, these cracks cannot lead to corrosive media passing through the deposited thin film.

The characteristics of the optimized sample were evaluated and the results are summarized in Figure 9 and Table 5. Figure 9-a shows count plates after anaerobic incubation for 4 days at 37 °C. It is clear that the deposited thin film acts as an antimicrobial barrier, prevents the survival and growth of SRB, postpones the formation of biofilm, and consequently restrains the microbiologically induced corrosion. The antibacterial performance of this sample was measured as ~ 60 %, confirming that the optimum conditions used for the sample preparation could be authentic. Figure 9-b and Table 5 show results of the Tafel polarization corrosion test for the optimized sample and the bare one. Although i_{corr} of this sample is not as low as that of sample 6, its corrosion resistance is extremely higher than the other coated and bare samples. The results show that the *Aim* value of the optimized sample is about 91% which is higher than the other samples.

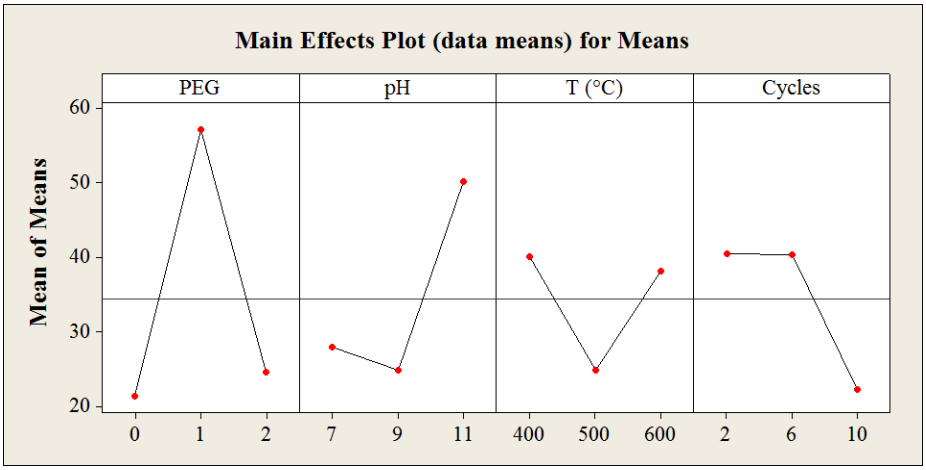

Figure 7. Main effects plot for S/N ratios of *Aim* parameter.

Table 5. Bactericidal efficiency and i_{corr} of the optimized sample

Sample	Optimized Sample	Uncoated Sample
Bactericidal efficiency (%)	60	3.6
i_{corr} ($\mu A.cm^{-2}$)	0.050	3.551

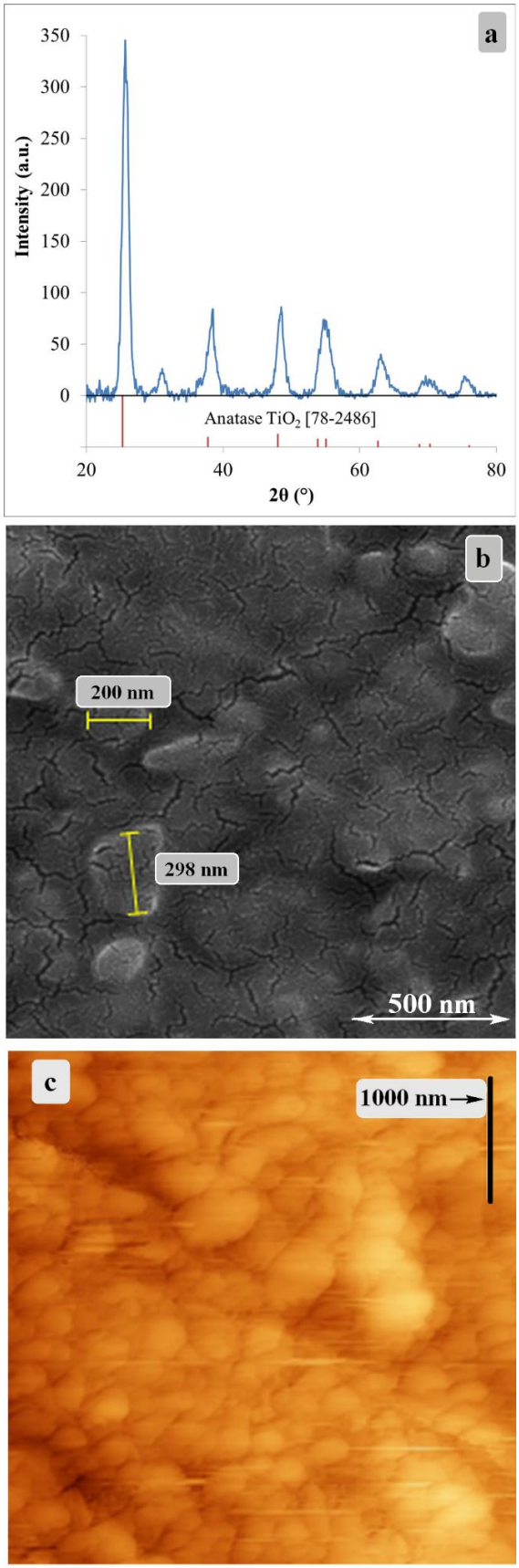

Figure 8. XRD pattern (a), SEM image (b), and AFM graph (c) of the as-prepared optimized sample.

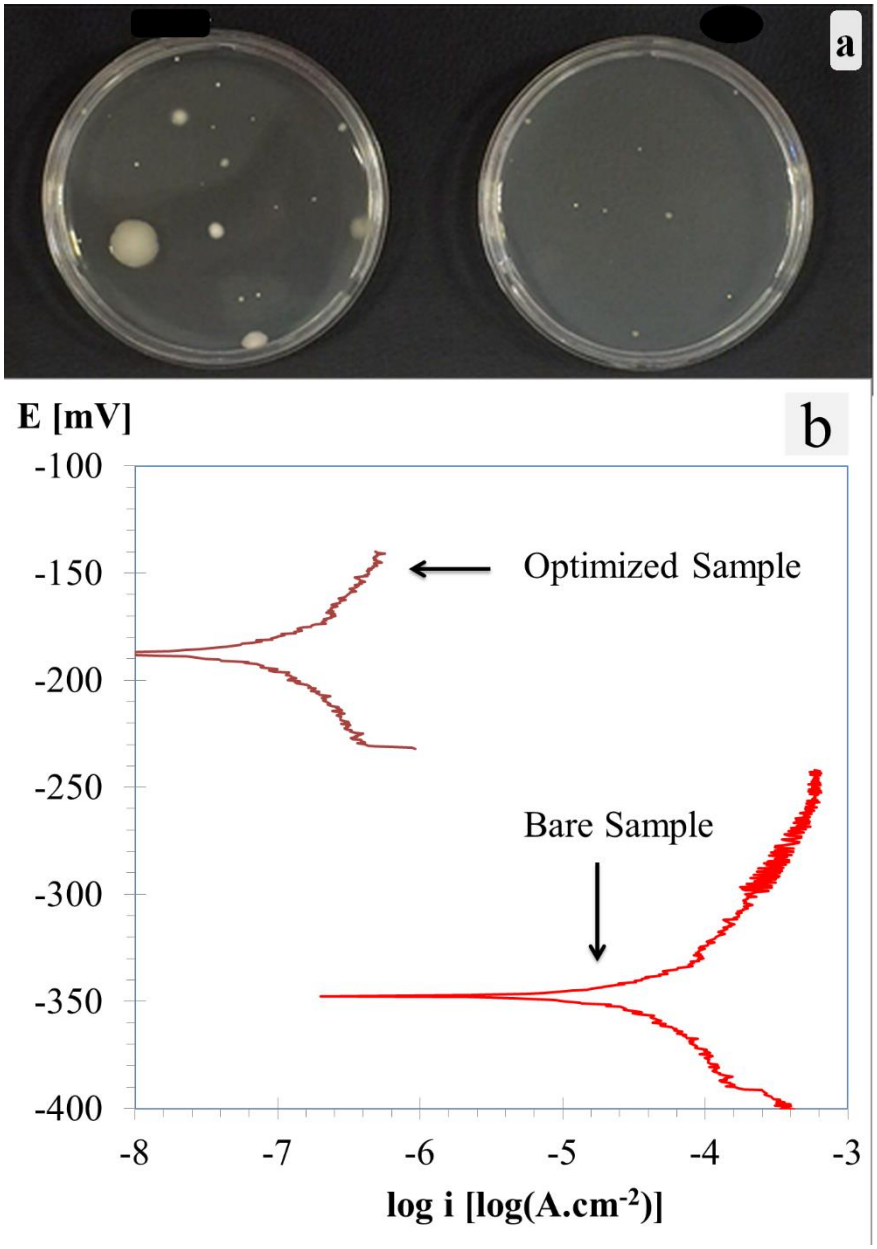

Figure 9. (a) Count plates after anaerobic incubation for 4 days at 37 °C. (b) Tafel polarization curves of the optimized sample.

4- Conclusions

The microbiologically induced corrosion of stainless steel was well controlled by deposition of TiO_2 thin film via sol gel dipping method. Taguchi methodology showed that PEG content and pH had the highest effects on the bactericidal efficiency and i_{corr}, respectively. The required conditions to achieve the highest *Aim* parameter value are: PEG content=1 g per 100 mL of sol, pH=11, T=600 °C, and dipping cycles=2. These conditions were used to prepare the optimized sample and to evaluate the prediction of Taguchi approach. In this sample, bactericidal efficiency increases and i_{corr} value decreases about 60 and 70 %, respectively. These results confirmed the prediction of Taguchi method and the highest *Aim* value was calculate about 90%.

References

[1] Y. Zhao, E. Zhou, Y. Liu, S. Liao, Z. Li, D. Xu, T. Zhang and T. Gu, "Comparison of different electrochemical techniques for continuous monitoring of the

microbiologically influenced corrosion of 2205 duplex stainless steel by marine Pseudomonas aeruginosa biofilm", Corrosion Science, Vol. 126, 2017, pp. 142-151.

[2] L. T. Popoola, A. S. Grema, G. K. Latinwo, B. Gutti and A. S. Balogun, "Corrosion problems during oil and gas production and its mitigation", International Journal of Industrial Chemistry, Vol. 4, 2013, pp. 35.

[3] B. Phull and A. A. Abdullahi, "Marine Corrosion," Reference Module in Materials Science and Materials Engineering. Elsevier, 2017.

[4] S. H. Oliveira, M. A. G. A. Lima, F. P. França, M. R. S. Vieira, P. Silva and S. L. Urtiga Filho, "Control of microbiological corrosion on carbon steel with sodium hypochlorite and biopolymer", International Journal of Biological Macromolecules, Vol. 88, 2016, pp. 27-35.

[5] T. Liu and Y. F. Cheng, "The influence of cathodic protection potential on the biofilm formation and corrosion behaviour of an X70 steel pipeline in sulfate reducing bacteria media", Journal of Alloys and Compounds, Vol. 729, 2017, pp. 180-188.

[6] P. Parthipan, J. Narenkumar, P. Elumalai, P. S. Preethi, A. Usha Raja Nanthini, A. Agrawal and A. Rajasekar, "Neem extract as a green inhibitor for microbiologically influenced corrosion of carbon steel API 5LX in a hypersaline environments", Journal of Molecular Liquids, Vol. 240, 2017, pp. 121-127.

[7] H. Liu, T. Gu, Y. Lv, M. Asif, F. Xiong, G. Zhang and H. Liu, "Corrosion inhibition and anti-bacterial efficacy of benzalkonium chloride in artificial CO2-saturated oilfield produced water", Corrosion Science, Vol. 117, 2017, pp. 24-34.

[8] L. L. Machuca, R. Jeffrey, S. I. Bailey, R. Gubner, E. L. J. Watkin, M. P. Ginige, A. H. Kaksonen and K. Heidersbach, "Filtration–UV irradiation as an option for mitigating the risk of microbiologically influenced corrosion of subsea construction alloys in seawater", Corrosion Science, Vol. 79, 2014, pp. 89-99.

[9] T. L. Skovhus, R. B. Eckert and E. Rodrigues, "Management and control of microbiologically influenced corrosion (MIC) in the oil and gas industry—Overview and a North Sea case study", Journal of Biotechnology, Vol. 256, 2017, pp. 31-45.

[10] M. Köller, P. Bellova, S. M. Javid, Y. Motemani, C. Khare, C. Sengstock, K. Tschulik, T. A. Schildhauer and A. Ludwig, "Antibacterial activity of microstructured sacrificial anode thin films by combination of silver with platinum group elements (platinum, palladium, iridium)", Materials Science and Engineering: C, Vol. 74, 2017, pp. 536-541.

[11] Y. Wang, D. Zhang and Z. Lu, "Hydrophobic Mg–Al layered double hydroxide film on aluminum: Fabrication and microbiologically influenced corrosion resistance properties", Colloids and Surfaces A: Physicochemical and Engineering Aspects, Vol. 474, 2015, pp. 44-51.

[12] B. González-Penguelly, Á. d. J. Morales-Ramírez, M. G. Rodríguez-Rosales, C. O. Rodríguez-Nava and M. L. Carrera-Jota, "New infrared-assisted method for sol-gel derived ZnO:Ag thin films: Structural and bacterial inhibition properties", Materials Science and Engineering: C, Vol. 78, 2017, pp. 833-841.

[13] N. O. San, H. Nazır and G. Dönmez, "Evaluation of microbiologically influenced corrosion inhibition on Ni–Co alloy coatings by Aeromonas salmonicida and Clavibacter michiganensis", Corrosion Science, Vol. 65, 2012, pp. 113-118.

[14] S. P. Tambe, S. D. Jagtap, A. K. Chaurasiya and K. K. Joshi, "Evaluation of microbial corrosion of epoxy coating by using sulphate reducing bacteria", Progress in Organic Coatings, Vol. 94, 2016, pp. 49-55.

[15] S. Naghibi, A. Jamshidi, O. Torabi and R. E. Kahrizsangi, "Application of Taguchi Method for Characterization of Corrosion Behavior of TiO2 Coating Prepared by Sol-Gel Dipping Technique", International Journal of Applied Ceramic Technology, Vol. 11, 2014, pp. 901-910.

[16] M. Pourmoalem and S. Naghibi, "Potency of commercial TiO2-P25 nanoparticles to form stainless steel protective coating", International Journal of Applied Ceramic Technology, Vol. 2017, pp. n/a-n/a.

[17] M. A. Deyab and S. T. Keera, "Effect of nano-TiO2 particles size on the corrosion resistance of alkyd coating", Materials Chemistry and Physics, Vol. 146, 2014, pp. 406-411.

[18] I. Poulios, P. Spathis, A. Grigoriadou, K. Delidou and P. Tsoumparis, "Protection of marbles against corrosion and microbial corrosion with TiO2 coatings", Journal of Environmental Science and Health, Part A, Vol. 34, 1999, pp. 1455-1471.

[19] B. M. Praveen and T. V. Venkatesha, "Electrodeposition and Corrosion Resistance Properties of Zn-Ni/TiO2 Nano composite Coatings", International Journal of Electrochemistry, Vol. 2011, 2011, pp.

[20] H. Wang, B. Tang, X. Li and Y. Ma, "Antibacterial Properties and Corrosion Resistance of Nitrogen-doped TiO2 Coatings on Stainless Steel", Journal of Materials Science & Technology, Vol. 27, 2011, pp. 309-316.

[21] H. Wang, Z. Wang, H. Hong and Y. Yin, "Preparation of cerium-doped TiO2 film on 304 stainless steel and its bactericidal effect in the presence of sulfate-reducing bacteria (SRB)", Materials Chemistry and Physics, Vol. 124, 2010, pp. 791-794.

[22] R. Basheer, G. Ganga, R. K. Chandran, G. M. Nair, M. B. Nair and S. M. A. Shibli, "Effect of W–TiO2 composite to control microbiologically influenced corrosion on galvanized steel", Applied Microbiology and Biotechnology, Vol. 97, 2013, pp. 5615-5625.

[23] J. Ma, Y. Shi, J. Di, Z. Yao and H. Liu, "Effect of TiO2 nanoparticles on anticorrosion property in amorphous Ni-P-Cr composite coating in artificial seawater and microbial environment", Materials and Corrosion, Vol. 60, 2009, pp. 274-279.

[24] Z. Xu, D. Jiang, Z. Wei, J. Chen and J. Jing, "Fabrication of superhydrophobic nano-aluminum films on stainless steel meshes by electrophoretic deposition for oil-water separation", Applied Surface Science, Vol. 427, 2018, pp. 253-261.

[25] P. Velusamy, R. Ramesh Babu, K. Ramamurthi, E. Elangovan, J. Viegas and M. Sridharan, "Spray deposited ruthenium incorporated CdO thin films for opto-electronic and gas sensing applications", Journal of Physics and Chemistry of Solids, Vol. 112, 2018, pp. 127-136.

[26] R. M. Kenzhin, Y. I. Bauman, A. M. Volodin, I. V. Mishakov and A. A. Vedyagin, "Synthesis of carbon nanofibers by catalytic CVD of chlorobenzene over bulk nickel alloy", Applied Surface Science, Vol. 427, 2018, pp. 505-510.

[27] J. L. Daure, K. T. Voisey, P. H. Shipway and D. A. Stewart, "The effect of coating architecture and defects on the corrosion behaviour of a PVD multilayer Inconel 625/Cr coating", Surface and Coatings Technology, Vol. 324, 2017, pp. 403-412.

[28] B. Xue, M. Yu, J. Liu, J. Liu, S. Li and L. Xiong, "Corrosion protection of AA2024-T3 by sol-gel film modified with graphene oxide", Journal of Alloys and Compounds, Vol. 725, 2017, pp. 84-95.

[29] R. Mechiakh, N. B. Sedrine, R. Chtourou and R. Bensaha, "Correlation between microstructure and optical properties of nano-crystalline TiO2 thin films prepared by sol–gel dip coating", Applied Surface Science, Vol. 257, 2010, pp. 670-676.

[30] A. J. Haider, R. H. Al– Anbari, G. R. Kadhim and C. T. Salame, "Exploring potential Environmental applications of TiO2 Nanoparticles", Energy Procedia, Vol. 119, 2017, pp. 332-345.

[31] B. Burnat, J. Robak, A. Leniart, I. Piwoński and D. Batory, "The effect of concentration and source of calcium ions on anticorrosion properties of Ca-doped TiO2 bioactive sol-gel coatings", Ceramics International, Vol. 43, 2017, pp. 13735-13742.

[32] L. Berthod, O. Shavdina, F. Vocanson, M. Langlet, O. Dellea, C. Veillas, S. Reynaud, I. Verrier and Y. Jourlin, "Colloidal photolithography applied to functional microstructure on cylinder based on photopatternable TiO2 sol-gel", Microelectronic Engineering, Vol. 177, 2017, pp. 46-51.

[33] E. Yücel, N. Güler and Y. Yücel, "Optimization of deposition conditions of CdS thin films using response surface methodology", Journal of Alloys and Compounds, Vol. 589, 2014, pp. 207-212.

[34] C. I. da Silva Oliveira, D. Martinez Martinez, A. Al-Rjoub, L. Rebouta, R. Menezes and L. Cunha, "Development of a statistical method to help evaluating the transparency/opacity of decorative thin films", Applied Surface Science, Vol. 2017, pp.

[35] C. S. Yoo and A. G. Dixon, "Factorial experimental investigation of plasma-enhanced chemical vapor deposition of silicon nitride thin films", Thin Solid Films, Vol. 168, 1989, pp. 281-289.

[36] G. Casalino, F. Curcio and F. Memola Capece Minutolo, "Investigation on Ti6Al4V laser welding using statistical and Taguchi approaches", Journal of Materials Processing Technology, Vol. 167, 2005, pp. 422-428.

[37] V. N. Gaitonde, S. R. Karnik, B. T. Achyutha and B. Siddeswarappa, "Taguchi optimization in drilling of AISI 316L stainless steel to minimize burr size using multi-performance objective based on membership function", Journal of Materials Processing Technology, Vol. 202, 2008, pp. 374-379.

[38] M. J. Davidson, K. Balasubramanian and G. R. N. Tagore, "Experimental investigation on flow-forming of AA6061 alloy—A Taguchi approach", Journal of Materials Processing Technology, Vol. 200, 2008, pp. 283-287.

[39] S. Naghibi, M. A. Faghihi Sani and H. R. Madaah Hosseini, "Application of the statistical Taguchi method to optimize TiO2 nanoparticles synthesis by the hydrothermal assisted sol–gel technique", Ceramics International, Vol. 40, 2014, pp. 4193-4201.

[40] A. Jamshidi, A. A. Nourbakhsh, S. Naghibi and K. J. D. MacKenzie, "Application of the statistical Taguchi method to optimize X-SiAlON and mullite formation in composite powders prepared by the SRN process", Ceramics International, Vol. 40, 2014, pp. 263-271.

[41] E. Katouei Zadeh, S. M. Zebarjad and K. Janghorban, "Optimization of synthesis conditions of N-doped TiO2 nanoparticles using Taguchi robust design", Materials Chemistry and Physics, Vol. 201, 2017, pp. 69-77.

[42] T. T. Ajaal and R. W. Smith, "Employing the Taguchi method in optimizing the scaffold production process for artificial bone grafts", Journal of Materials Processing Technology, Vol. 209, 2009, pp. 1521-1532.

[43] N. Kumari, J. V. Gohel and S. R. Patel, "Multi-response optimization of ZnO thin films using Grey-Taguchi technique and development of a model using ANN", Optik - International Journal for Light and Electron Optics, Vol. 144, 2017, pp. 422-435.

[44] H.-C. Chuang and W.-F. Lee, "Parametric optimization of Nd–YVO4 laser for straight scribing on silver

nanowire based conductive thin films by Taguchi method", Optics & Laser Technology, Vol. 57, 2014, pp. 149-153.

[45] N. I. o. Standards, Technology and I. SEMATECH., NIST/SEMATECH Engineering Statistics Handbook, 2002

[46] T.-C. Cheng, K.-S. Yao, Y.-H. Hsieh, L.-L. Hsieh and C.-Y. Chang, "Optimizing preparation of the TiO2 thin film reactor using the Taguchi method", Materials & Design, Vol. 31, 2010, pp. 1749-1751.

[47] S. Pourjafar, M. Jahanshahi and A. Rahimpour, "Optimization of TiO2 modified poly(vinyl alcohol) thin film composite nanofiltration membranes using Taguchi method", Desalination, Vol. 315, 2013, pp. 107-114.

[48] W. J. Yang, C. Y. Hsu, Y. W. Liu, R. Q. Hsu, T. W. Lu and C. C. Hu, "The structure and photocatalytic activity of TiO2 thin films deposited by dc magnetron sputtering", Superlattices and Microstructures, Vol. 52, 2012, pp. 1131-1142.

[49] N. Tasić, Z. Branković, Z. Marinković-Stanojević and G. Branković, "Effect of Binder Molecular Weight on Morphology of TiO2 Films Prepared by Tape Casting and their Photovoltaic Performance", Science of Sintering, Vol. 44, 2012, pp.